Eur. J. Entomol. **108**: 25–34, 2011
http://www.eje.cz/scripts/viewabstract.php?abstract=1583
ISSN 1210-5759 (print), 1802-8829 (online)

Recombinant expression, purification and characterization of *Bombyx mori* (Lepidoptera: Bombycidae) pyridoxal kinase

SHUO-HAO HUANG[1, 2], WANG MA[1], PING-PING ZHANG[3], JIAN-YUN ZHANG[3], YAN-FENG XIE[1] and LONG-QUAN HUANG[1]*

[1] Key Laboratory of Tea Biochemistry & Biotechnology of Ministry of Education and Ministry of Agriculture, Anhui Agricultural University, Hefei 230036, People's Republic of China

[2] Graduate School of Systems Life Sciences, Kyushu University, 744 Motooka, Nishi-ku, Fukuoka 819-0395, Japan

[3] College of Life Science, Anhui Agricultural University, Hefei 230036, People's Republic of China

Key words. *Bombyx mori*, pyridoxal kinase, recombinant expression, purification, characterization

Abstract. Pyridoxal kinase (PLK; EC 2.7.1.35) is a key enzyme in the metabolism of vitamin B_6 (VB_6) in *Bombyx mori*. A fusion expressional vector pET-22b-BPLK-His was constructed using a sub-cloning technique, the recombinant *B. mori* PLK was then expressed in *Escherichia coli*, purified and characterized. Bioinformatics were used to deduce the protein structure and genomic organization of this enzyme. Using Ni Sepharose affinity column chromatography, the recombinant protein was purified to very high degree (approximately 90%). The recombinant PLK exhibits a high specific enzymatic activity (1800 nmol/min/mg of protein). The maximum catalytic activity of this enzyme was recorded over a narrow pH range (5.5–6.0) and Zn^{2+} is the most effective cation for catalysis under saturating substrate concentrations. When only triethanolamine is present as the cation, K^+ is an activator of PLK. A double reciprocal plot of initial velocity suggests that the enzyme catalyses the reaction by means of a sequential catalytic mechanism. Under optimal conditions, the *K*m value for the substrates of ATP and pyridoxal are 57.9 ± 5.1 and 44.1 ± 3.9 μM. *B. mori*'s genome contains a single copy of the *PLK* gene, which is 7.73 kb long and contains five exons and four introns, and is located on the eighth chromosome. The PLK may be a dimer with two identical subunits under native conditions, and it is hypothesized that each monomer contains eight α-helices (α1-8), nine β-strands (β1-9) and two segments of 3_{10} helices.

INTRODUCTION

Vitamin B_6 (VB_6) exists in various forms, pyridoxal (PL), pyridoxine (PN), pyridoxamine (PM) and their phosphorylated derivatives: Pyridoxal 5'-phosphate (PLP), pyridoxine 5'-phosphate (PNP) and pyridoxamine 5'-phosphate (PMP). PLP is the active form of VB_6 and acts as an essential, ubiquitous coenzyme in many aspects of amino acid and cellular metabolism. The de novo biosynthesis of VB_6 takes place in microorganisms and plants, but animals have lost this ability and it is essential they include it in their diet for the biosynthesis of PLP via a salvage pathway. In the salvage pathway, pyridoxal kinase (PLK) (EC 2.7.1.35) catalyzes the ATP-dependent phosphorylation of PL, PM and PN to form PLP, PMP and PNP, respectively. PNP and PMP are oxidized to form PLP by pyridoxine 5'-phosphate oxidase (PNPO; EC 1.4.3.5).

PLKs from bacteria and mammals have been purified and characterized (White & Dempsey, 1970; Kwok & Churchich, 1979; Kerry et al., 1986; Kerry & Kwok, 1986; Kwok et al., 1987; Sakurai et al., 1993). The gene encoding PLK has been isolated from mammals (Hanna et al., 1997; Gao et al., 1998; Maras et al., 1999), microorganisms (Yang et al., 1996, 1998; Scott & Phillps, 1997) and plants (Lum et al., 2002; Wang et al., 2004). Several mammalian PLKs have been successfully expressed in *Escherichia coli* and the expressed recombinant proteins exhibit the same biochemical characteristics as those of the native protein purified from various mammalian tissues (Gao et al., 1998; Lee et al., 2000; Di Salvo et al., 2004). Recently, the three-dimensional structures of PLKs from bacteria and mammals, alone and in complex with various ligands were determined, providing a better understanding of the catalytic mechanism of PLK (Li et al., 2002, 2004; Safo et al., 2004, 2006; Tang et al., 2005; Cao et al., 2006). The active sites are structurally very similar among members of the ribokinase superfamily (Zhang et al., 2004). Therefore, the location and mode of substrate binding in human PLK have been deduced by analogy with the structures of sheep brain PLK in complex with various substrates (Cao et al., 2006).

Like mammals, insects rely on a nutritional source of VB_6 to synthesize PLP. When newly moulted larvae of *Bombyx mori* are reared on a VB6-deficient diet, almost all of them died before moulting to the next instar (Huang et al., 1998). While the biological function of VB_6 is similar in all organisms, there are differences between insects and mammals in VB_6 metabolism. In mammals, PLP is first synthesized in the liver and then released into the bloodstream in association with albumin. Circulating PLP is dephosphorylated by membrane-associated phosphatase to gain entry into cells and is then converted back

* Corresponding author; e-mail: lqhuang218@yahoo.com.cn

to PLP by intracellular PLK (Lumeng et al., 1980; Merrill et al., 1984). In a previous study on VB_6 metabolism in *B. mori* larvae, it was found that dietary PN is absorbed by the midgut, then diffuses into the hemolymph and is actively transported to other organs. PN is first phosphorylated to PNP by PLK, which is then oxidized to PLP by PNPO in every larval organ except hemolymph (Zhang & Huang, 2003). Since *B. mori* is a large silk-secreting insect, its immense protein turnover needs the timely support of PLP. In order to understand the metabolic mechanism of VB_6 in *B. mori*, the cDNAs encoding PLK and PNPO in *B. mori* larvae were cloned (Shi et al., 2007; Huang et al., 2009). In this study, the recombinant *B. mori* PLK was expressed in *E. coli* as a fusion protein with a hexa-histidine affinity tag, purified by Ni Sepharose affinity column chromatography and characterized. The genomic organization and protein structure of *B. mori* PLK were also deduced by bioinformatics.

MATERIAL AND METHODS

Material

The *B. mori* PLK gene was from the vector pET-22b-BPLK, which was constructed in our laboratory (GenBank accession number: DQ452397). The *E. coli* strains Rosetta (DE3) and DH5α, and pfu DNA polymerase were purchased from Beijing TransGen Biotech (Beijing, China). Restriction enzymes (*Nde* I, *Xho* I), and T4 DNA ligase were purchased from TaKaRa (Dalian, China). A Gel Extraction Kit (SK1131), SYBR Green I, Isopropyl-β-D-thiogalactopyranoside (IPTG), DNA marker, protein marker, Coomassie brilliant blue G250/R250 and all other general reagents, were purchased from Sangon (Shanghai, China). Protease inhibitor cocktails, PLP, PMP-HCl, PNP, PL-HCl, PM-2HCl and PN-HCl were purchased from Sigma-Aldrich (Shanghai, China). Ni Sepharose 6 Fast Flow and Millipore columns were purchased from GEHC (Shanghai, China) and Kenqiang (Shanghai, China), respectively. The primer construction was completed by Sangon Bio-technology Company (Shanghai, China).

Gene subcloning

Using pET-22b-BPLK as a template, the full coding region of the *BPLK*-gene was obtained by PCR reaction. The PCR reaction had a total volume of 50 μL, containing 1 μL of templates, 5 μL of 10 × buffer, 200 μM of each dNTP, 300 nM of each primer, 5 U of pfu DNA polymerase and ddH_2O 39 μL. To take out the terminator contained in the coding region of *BPLK*, primers used in the PCR were as follows: sense primer (5'-GGCCATATGTCTCAAGATGATACTCCA-3') and anti-sense primer (5'-GTCTCTCGAGGTTTATTTTCACAGCCTT-3'), which contained *Nde* I and *Xho* I recognition sites (underlined). Amplification was performed in a thermal-cycler (Y-Gradient Thermoblock, Biometra, Germany) as follows: 5 min at 94°C; 30 cycles of 30 s at 94°C, 30 s at 55°C and 60 s at 72°C, followed by 10 min at 72°C. The PCR product was purified using DNA Gel Extraction kit, and digested with *Nde* I and *Xho* I restriction enzymes. The digested fragment was then purified again and ligated with T4 DNA ligase into pET-22b(+), previously digested with the same enzymes. The resulting recombinant plasmid was named pET-22b-BPLK-His, which contained a T7 promoter, *B. mori PLK* gene fused to a C-terminal hexa-histidine affinity tag sequence and T7 terminator.

The plasmid was used to transform the competent cells of *E. coli* DH5α for sequencing. The sequencing study was accomplished by Sangon Bio-technology Company (Shanghai, China) using the dye terminator method and an ABI 3730 automatic DNA sequencer.

Protein expression and purification

After the electrophoretic analysis and sequencing analysis of the DNA fragment, pET-22b-BPLK-His was used to transform *E. coli* Rosetta (DE3) cells for protein expression. The single bacterial colony of *E. coli* Rosetta (DE3), harbouring pET-22b-BPLK-His, was cultured in 20 mL Luria-Bertani (LB) medium with ampicillin (50 μg/mL) and chloramphenicol (3.4 μg/mL) on a shaker platform, overnight, at 37°C, and 4 mL of the overnight cultures was then inoculated into 400 mL LB medium with ampicillin (50 μg/mL) and chloramphenicol (3.4 μg/mL). The inoculum was grown at 37°C with vigorous shaking to an OD_{600}, approximately 0.4–0.6. IPTG was added to a final concentration of 1.0 mM and the cells further incubated and shaken for 12 h at 16°C. Cells were harvested by centrifugation (6,347 × g at 4°C for 15 min), re-suspended in cold 1 × phosphate-buffered saline (PBS) (10 mM sodium phosphate, pH 7.4, 140 mM sodium chloride, 5 mM potassium chloride) and collected by centrifugation (6,347 × g at 4°C for 15 min).

The pellets were re-suspended in loading buffer (20 mM sodium phosphate, pH 7.4, 20 mM imidazole, 0.5 M NaCl). Protease inhibitor cocktails were added according to the manufacturer's instruction. Unless otherwise specified, all subsequent steps were performed at 4°C. The suspensions were then broken up by sonication in ice and centrifuged at 12,840 × g for 10 min.

For the purification, about 10 mL of the supernatant was loaded onto a chromatography column (24 mL) filled with 3 mL of Ni Sepharose and washed extensively with sodium phosphate buffer with increased imidazole concentration (= 150 mM) to remove un-specifically bound proteins, including *E. coli* PLK. Subsequently the histidine-tagged protein was eluted in 16 mL of sodium phosphate buffer containing 300 mM imidazole. The purified *B. mori* PLK was concentrated to about 0.42 mg/mL with a Millipore (10,000 Da cut-off) in a buffer of 70 mM potassium phosphate, pH 6.5. The above description is of a typical run.

The purity and homogeneity of the fractions and the subunit molecular weight of the PLK were estimated by 1-dimensional SDS-PAGE. Protein concentrations were determined by the method of Bradford using bovine serum albumin as standard. The molecular weight was determined by injecting approximately 3 mg purified *B. mori* PLK into a Sephadex G-100 column (1 × 100 cm). Samples of lysozyme, chymotrypsinogen, ovalbumin and hemoglobin were used as markers of known molecular weight. The elution buffer was 50 mM Tris-HCl (pH 7.5) and the flow rate 0.4 ml/min.

Assay of PLK activity

Using PL as a substrate PLK activity was determined using the method of Sakurai (Sakurai et al., 1993) with some modifications. The formed product, PLP was determined by reaction with phenylhydrazine to enhance the sensitivity. Unless otherwise specified, all activity assays were performed three times. Purified enzyme (about 12 μg) was incubated at 37°C for 10 min in an assay buffer of 70 mM potassium phosphate (pH 5.5) with 1.0 mM PL, 1.0 mM ATP and 0.5 mM $ZnCl_2$ in a total volume of 1 mL. The reaction was stopped by adding 100 μL of 100% (w/v) trichloroacetic acid, centrifuged at 11,400 × g for 10 min and any precipitate that formed discarded. One hundred micro liters of phenylhydrazine in 10 M sulphuric acid was added to the mixture of 1 mL of supernatant and 2 mL of assay buffer. Enzyme activity was determined using a spectrophotometer at 410 nm for the first 2.5 min (Unico UV-2600 spectrophotometer, Unico instrument Co., Ltd, shanghai, China). The

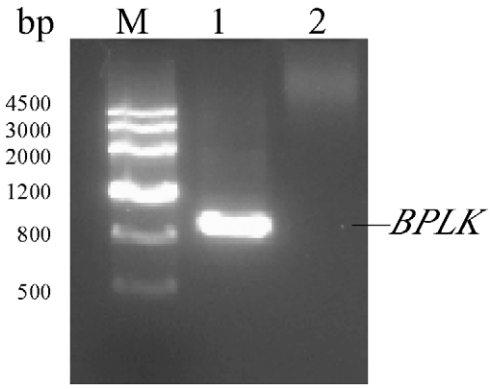

Fig. 1. Electrophoresis of the products of colony PCR. Lane M is DNA marker; Lane 1 is *BPLK*; Lane 2 is negative control.

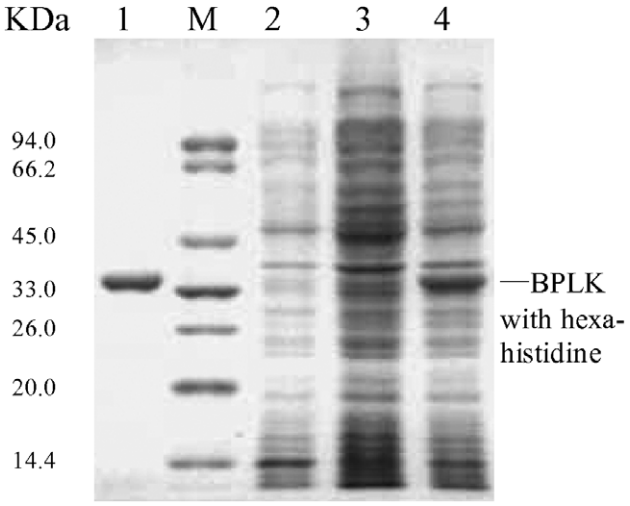

Fig. 2. SDS-PAGE (12%) analysis of the recombinant *B. mori* PLK. Lane 1 is purified recombinant *B. mori* PLK; Lane M is molecular weight standard; Lane 2 is crude extract of *E. coli* Rosetta (DE3) harbouring pET22b(+); Lane 3 and 4 are crude extracts of *E. coli* Rosetta (DE3) harbouring pET22b-BPLK-His, induced by IPTG after 0 h and 12 h, in that order.

blank was prepared by adding ATP after stopping the reaction with trichloroacetic acid. A unit of activity is defined as the nmol of PLP formed per minute per mg of protein at 37°C. A standard curve of the absorbance at 410 nm against different concentrations of PLP standard was constructed for calculating the PLP generated in the enzyme assay.

The pH dependence of the PLK activity was measured between pH 4 and 9, with an assay buffer of 70 mM citric acid/potassium orthophosphate/boric acid solutions adjusted with NaOH. Activity assays were performed at various pHs at 37°C for 10 min. The effect of temperature on the PLK activity and stability were determined at temperatures from 20 to 55°C. Activity was measured for 10 min at different temperatures. For stability assays, the enzyme was pre-incubated for 1 h at the indicated temperature, and residual activity was then assayed at 37°C as described above. Effect of divalent cations on the activity of the PLK was measured in the standard assay condition with 0.5 mM of various divalent cations instead of $ZnCl_2$.

To compute the enzyme kinetic data, about 10 μg of the purified enzyme was used in each assay, and the concentrations of substrates were varied in the range 2-800 μM. At this enzyme concentration, the initial enzymatic rate was linear. Using PL as the variable substrate and ATP as the fixed substrate, the enzyme kinetic mechanism was estimated from double reciprocal plots.

Analysis of genomic organization and protein structure of the enzyme

The *B. mori* PLK cDNA (GenBank accession number: DQ452397) was used as the query to search the genomic database of *B. mori* (http://www.silkdb.org/, http://sgp.dna.affric.go.jp/) for the gene, and the gene structure was analyzed using software SeqVISTA (http://www.bio-soft.net/format.html).

Software Clustal W (http://www.ebi.ac.uk/clustalw/) was used to align amino acid sequences of PLKs from *B. mori*, humans, sheep, *Arabidopsis thaliana*, wheat and *E. coli*, whose PLK activities have been confirmed. These sequences have the following database accession numbers: *B. mori*, (GenBank) DQ452397; humans, (GenBank) U89606; sheep, (Swiss-Prot) P82197; *A. thal*, (GenBank) AF404865; wheat, (GenBank) AY33732 1; *E coli*, (Swiss-Prot) P40191.

The secondary structure of the purified PLK was quantitatively determined by circular dichroism (CD) spectrum analysis. Determination of CD spectrum was carried out on a JASCO-J810 spectropolarimeter (Jasco Corporation, Japan). The instrument conditions were as follows: measurement range, 260–190 nm; data pitch, 0.2 nm; data points, 351; band width, 3 nm; response, 1 s; sensitivity, standard; scanning speed, 100 nm/min; accumulation, 3; cell length, 0.1 cm; temperature, room temperature; control and analysis software, Spectra Managermr. The purified PLK was dissolved in 50 mM potassium phosphate (pH 7.4) buffer with a concentration of 0.1 mg/mL.

The three-dimensional structure of *B. mori* PLK monomer was predicted by the method of homology modelling, using the human PLK (PDB accession number: 2YXT) as a template. Amino acid sequence was submitted to SWISS-MODEL server (http://www.swissmodol.expasy.crg/) for homology modelling. The result was analyzed by visual software Pymol (http://www.bio-soft.net/3d/pymol.htm). The location and mode of substrate binding in *B. mori* PLK was deduced by analogy with the known crystal structures of mammalian PLK in complex with substrates.

RESULTS

Recombinant expression and purification of *B. mori* PLK

With the help of colony PCR, about a 900 bp product was obtained from fusion expressional vector pET-22b-BPLK-His (Fig. 1). DNA sequencing demonstrated that the PCR product had a *B. mori PLK* gene and a C-terminal hexa-histidine tag sequence.

TABLE 1. Summary of the purification of recombinant *B. mori* PLK.

Fraction	Volume (mL)	Total protein (mg)	Protein concentration (mg/mL)	Total activity (nmol/min)	Activity (nmol/min/mL)	Specific activity (nmol/min/mg)
Crude preparation	10	17.9	1.79	1253	125.3	70
Purification	1.3	0.57	0.44	1029	792	1800

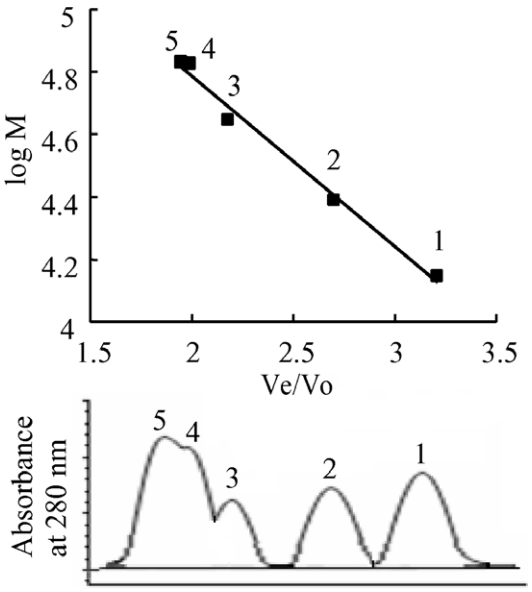

Fig. 3. Estimation of the molecular mass (M, kDa) of *B. mori* PLK by gel filtration using Sephadex G-100. 1 – lysozyme (14 kDa); 2 – chymotrypsinogen (25 kDa); 3 – ovalbumin (44 kDa); 4 – hemoglobin (67 kDa); 5 – *B. mori* PLK. Ve – elution volume; Vo – outer volume.

Using the polyhistidine as a fusion tag, the over expressed protein was found in the soluble fraction. Using Ni Sepharose affinity column chromatography, the PLK was purified to over 90% homogeneity judged from 1-dimensional SDS-PAGE analysis (Fig. 2). Table 1 summarizes the purification of PLK. The enzyme was purified about 26-fold, and the final yield of the enzyme was 82% of the homogenate activity.

The dimeric PLK molecular mass was determined to be 68 kDa by Sephadex G-100 gel filtration (Fig. 3). On a reducing SDS-PAGE gel (Fig. 2), the PLK, including one

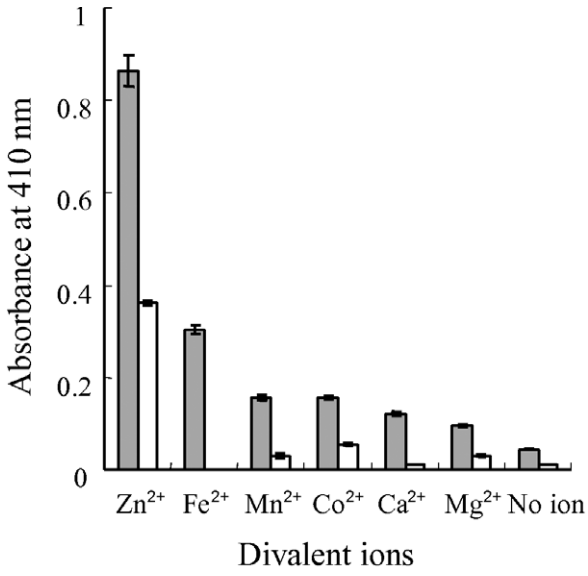

Fig. 5. Effect of divalent cation on the activity of the recombinant *B. mori* PLK. Filled column – activity assay with phosphate buffer (pH 5.5); open column – activity assay with triethanolamine buffer (pH 7.3).

6 × histidine tag in the C-terminus, appeared as a single band of about 33.9 kDa computed by software of Quantity one (http://www.seekbio.com/soft/275.html) based on the protein marker. The data suggest that the recombinant PLK is a dimer with two identical subunits under native conditions.

Catalytic properties of recombinant *B. mori* PLK

Fig. 4 shows the effect of pH on the catalytic activity of the purified PLK. The PLK has maximum catalytic activity in the narrow pH range of 5.5–6.0 and with Zn^{2+}, and the enzyme was inactive below pH 4.5. Enzyme activity decreased slowly above pH 6.0, to approximately

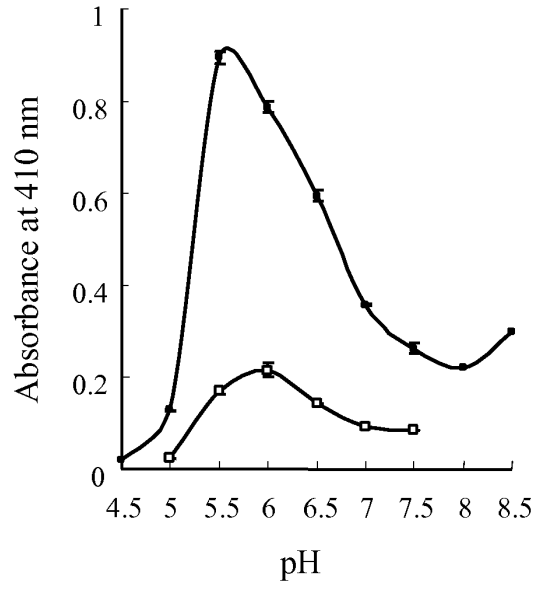

Fig. 4. Effect of pH on the catalytic activity of the recombinant *B. mori* PLK. Filled square – pH dependent assay with Zn^{2+}, and open square – pH dependent assay with Mg^{2+}.

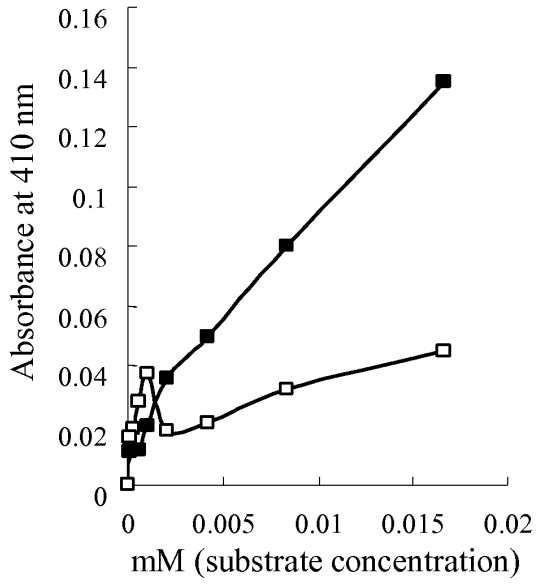

Fig. 6. Effect of Zn^{2+} and Mg^{2+} at different physiological substrate concentrations on the activity of the recombinant *B. mori* PLK. Filled square – Zn^{2+}; open square – Mg^{2+}.

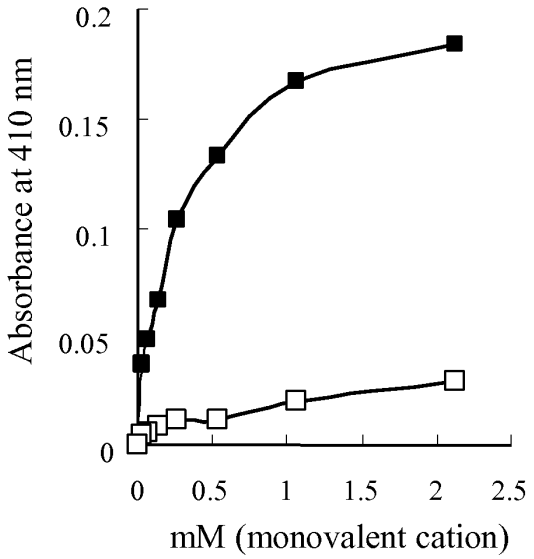

Fig. 7. Activity of *B. mori* PLK in the presence of either K^+ or Na^+. Monovalent cation was added in increasing concentrations to the PLK in triethanolamine buffer (pH 7.3). Filled square – K^+; open square – Na^+.

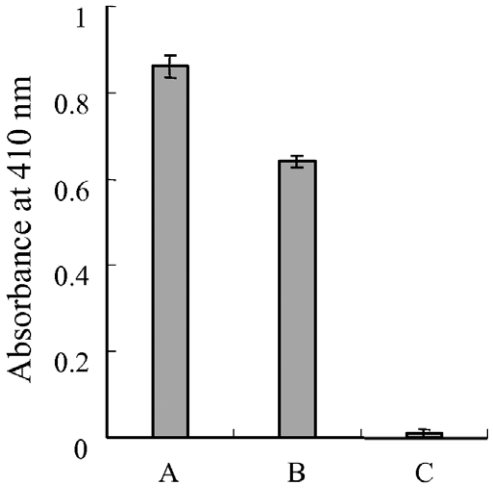

Fig. 8. Assays of *B. mori* PLK activity using 70 mM, pH 5.5 sodium phosphate buffer (A), sodium acetate buffer (B) and sodium citrate buffer (C).

35% at pH 8.5. Performing the pH dependent assay with Mg^{2+}, the optimum pH for the PLK activity was 6.0. The enzyme displayed optimal activity at 50°C, and its greatest stability was below 40°C (data not shown). At pH 5.5 and 37°C, the time course of enzyme activity was linear for up to 40 min (data not shown).

Figs 5 and 6 show the effect of divalent cation on PLK activity. Under saturating PL and ATP concentrations, Zn^{2+} is the most efficient cation for catalysis, analyzed with phosphate buffer (pH 5.5) or triethanolamine buffer (pH 7.3). At about a 1 μM substrate concentration, Mg^{2+}, however, stimulates the activity (Fig. 6). Enzyme activity was also measured using a monovalent cation at saturating PL and ATP concentrations, which revealed that K^+ is an activator of PLK when only triethanolamine is present as the cation (Fig. 7). If instead of the phosphate buffer an acetate buffer is used, enzymatic activity was reduced to 74% and almost no activity was recorded when a citrate buffer was used (Fig. 8).

An initial velocity study using PL as the variable substrate and ATP as the fixed substrate gave a family of lines intersecting to the left of the vertical axis (Fig. 9), which eliminated the possibility of a ping-pong catalytic mechanism. Such an intersecting pattern suggests that the enzyme catalyzes the reaction by means of a sequential catalytic mechanism. As the point of intersection of the lines is below the horizontal axis, it reveals that the combination of fixed substrate and enzyme affects the *K*m value of the variable substrate, which increases with increase in the concentration of the fixed substrate. Under optimal conditions, the *K*m values of PLK for ATP and PL were determined as 57.9 ± 5.1 and 44.1 ± 3.9 μM. Table 2 summarizes the kinetic parameters of PLK including the *K*m, *V*max, *k*cat and *k*cat/*K*m.

Genomic organization of *B. mori* PLK

Using cloned *B. mori* PLK cDNA as a query to search against the *B. mori* genomic database (http://www.silkdb.org/), the *PLK* gene was located at nscaf2828:3863864-3871593 with gene number BGIBMGA005472-TA. From the other *B. mori* genomic database (http://sgp.dna.affric.go.jp/), the *PLK* gene was located at chr8:11034281-11042010Bm_scaf19:3870164-3877893 with gene number BGIBMGA005472. The two genomic databases gave the same result. *B. mori* contains a single copy of the *PLK* gene on the eighth chromosome and no other homologous genes were found. The *PLK* gene spans a region about 7.73 kb long, and contains five exons and four introns (Fig. 10). Within the region from –26 to –68, relative to the transcription start site (-CCATAT-), typical TATA-like and CAAT-like boxes are identified. All exon/intron boundaries contain the canonical 5' donor GT and 3' acceptor AG sequences. At the 3' region of the *PLK* gene, some A-tailing sequences were identified.

TABLE 2. Kinetic data of recombinant *B. mori* PLK.

Substrate	*K*m (μM)	*V*max (μmol PLP min^{-1} mg^{-1})	*k*cat (S^{-1})	*k*cat/Km (M^{-1} S^{-1})
ATP	57.9 ± 5.1	2.23 ± 0.25	1.23	2.12×10^4
PL	44.1 ± 3.9	2.45 ± 0.28	1.35	3.06×10^4

Assay conditions were 2.0 mM fixed substrate, 2-800 μM variable substrate, 0.5 mM $ZnCl_2$, 70 mM potassium phosphate (pH 5.5), 10 μg of protein, at 37°C for 10 min.

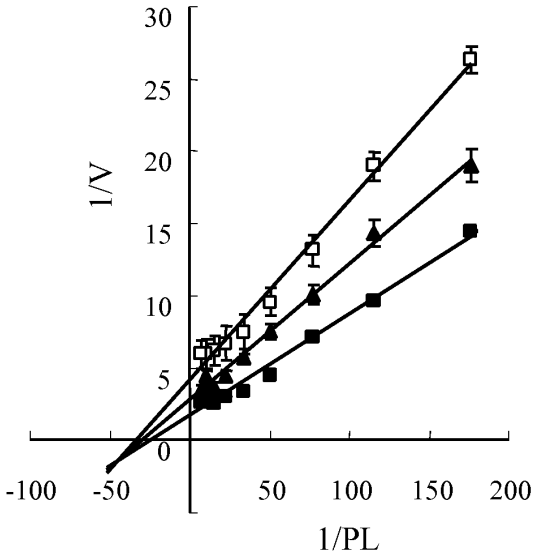

Fig. 9. Kinetic analysis of recombinant *B. mori* PLK. Using PL as the variable substrate and ATP as the fixed substrate. Open square – 0.04 mM ATP; filled triangle – 0.2 mM ATP; filled square – 1 mM ATP.

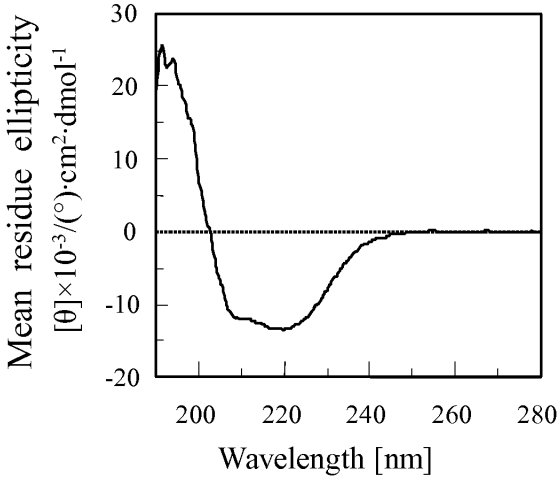

Fig. 11. Circular dichroism spectrum of recombinant *B. mori* PLK.

coli, respectively. *B. mori* PLK contains conserved amino acid sequence motifs that may be involved in substrate binding or catalysis of the PLK family. A distinctive characteristic of *B. mori* PLK is that its sequence is 10 or

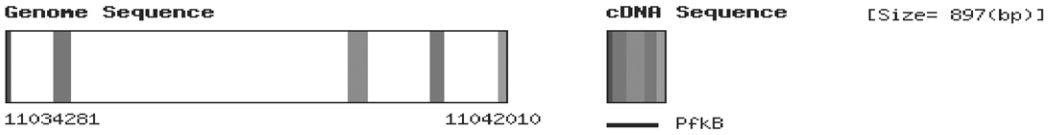

Fig. 10. Schematic diagram of the exon / intron organization of *B. mori* PLK gene obtained from *B. mori* genomic database (http://sgp.dna.affric.go.jp/).

Protein structure of *B. mori* PLK

Fig. 11 shows the circular dichroism spectra of the purified PLK. The relative percentage content of each secondary structure was: 43.1 ± 3.5% α-helix, 18.5 ± 2.3% β-sheet, 14.7 ± 0.8% β-turn and 23.6 ± 1.1% random coil respectively, computed by the circular dichroism spectrometer's software. The secondary structure content matched the theoretical analysis by software Psipred, which reveals that the purified PLK was not mis-folded. The secondary structure content of *B. mori* PLK is also similar to that of mammalian PLKs with three-dimensional structures (Table 3).

Fig. 12 shows the amino acid sequence alignment of *B. mori*, human, sheep, *A. thaliana*, wheat and *E. coli* PLKs. The *B. mori* PLK contains 298 amino acid residues with a theoretical molecular mass of 33.1 kDa and pI value of about 6.3. The amino acid sequence shares a 50% identity with that of human PLK, and 48% with sheep, 46.7% with *A. thaliana*, 44.48% with wheat and 32% with *E.* more residues shorter than that of PLK from mammals and plants. Compared with *B. mori* PLK, the sequence exhibits extension of the N-terminal in plants, and increase in nonconservative residues in mammal. Secondly, the key peptide loop, which is thought to play a significant role in the functioning of PLK (Safo et al., 2006), consists of eight residues in *B. mori* PLK and 12 in mammals.

Fig. 13 (B) shows the monomer structure of *B. mori* PLK, predicted using homology modelling, with the help of software Pymol (http://www.bio-soft.net/3d/pymol.htm). Each monomer consists of eight α-helices (α1–8), nine β-strands (β1–9) and two segments of 3_{10} helices. The 1–8 β-strands constitute a central contorted β-sheet flanked by α2, α3, α4, α5 and α6 on one side, and α1, α7 and α8 on the other side. The overall folding pattern is a αβα three-layer sandwich, which is common in the ribokinase super-family.

TABLE 3. Comparison of the secondary structure components of human, sheep, *E. coli* and *B. mori* PLKs.

Species	PDB accession number	amino acid residues	α-helix	β-sheet	β-turn and random coil
Human*	2YXT	312	38%	19%	43%
Sheep*	1LHP	312	39%	18%	43%
*B. mori***		298	42%	19%	39%

* With known crystal structure; ** Predicted by software Psipred (http://bioinf.cs.ucl.ac.uk/psipred/)

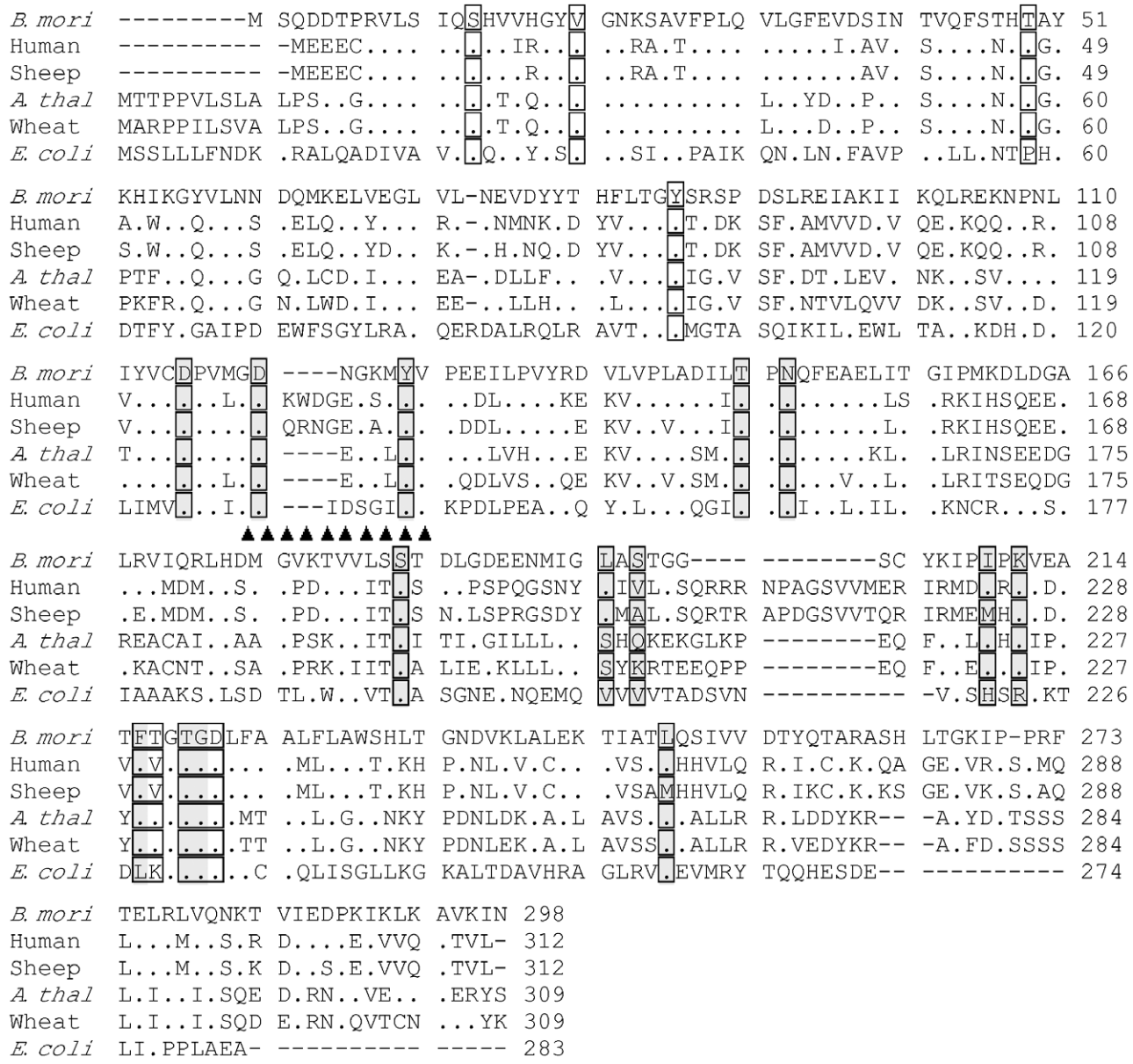

Fig. 12. Sequence alignment of PLKs from *B. mori*, humans, sheep, *A. thaliana*, wheat and *E. coli*. Dots for identical residues, dashes gaps introduced to maximize similarity. The key peptides of loop are marked by filled triangles. ATP-binding site and PL-binding site are boxed, and ATP-binding site is coloured grey.

Fig. 13 (C) shows the location and mode of substrate binding in *B. mori* PLK deduced by analogy with the structures of sheep brain PLK in complex with various substrates (Li et al., 2002, 2004). On the enzyme surface, there is a cavity with a negative charge located along one edge of the central β-sheet and this high negative charge attracts substrates with a positive charge, such as the pyridine ring of VB_6 and the adenine ring of ATP, which bind there. The ATP-binding site is positioned in a shallow groove formed by the hydrophobic side chains of surrounding residues. Residues that interact with the phosphate groups of ATP are Ser^{185}, Thr^{146}, Asp^{115}, Asn^{148}, Asp^{120}, Gly^{220}, Tyr^{125} and Thr^{219}; and residues Leu^{197}, Lys^{211}, Phe^{216}, Ser^{199}, Ile^{209} and Leu^{249} interact with the adenine ring of ATP. The PL-binding site is located in a pocket in the opposite direction of ATP, and consists of Tyr^{86}, Val^{21}, Thr^{217}, Ser^{14}, Thr^{49} and Asp^{221}.

DISCUSSION

A large number of genes/cDNAs encoding PLK have been isolated from mammals, microorganisms and plants, and their sequences submitted to the GenBank. A sequence homology search using the Dnaman program found several close homologs of PLK, from both prokaryotes and eukaryotes. The sequence identity with the human enzyme ranges from 24% to 90%. The amino acid sequence of *B. mori* PLK shares a 50% identity with that of human PLK.

In mammals, PLK is a dimer of identical subunits, each with an estimated molecular mass of approximately 35 kDa. The dimer can dissociate reversibly into catalytically

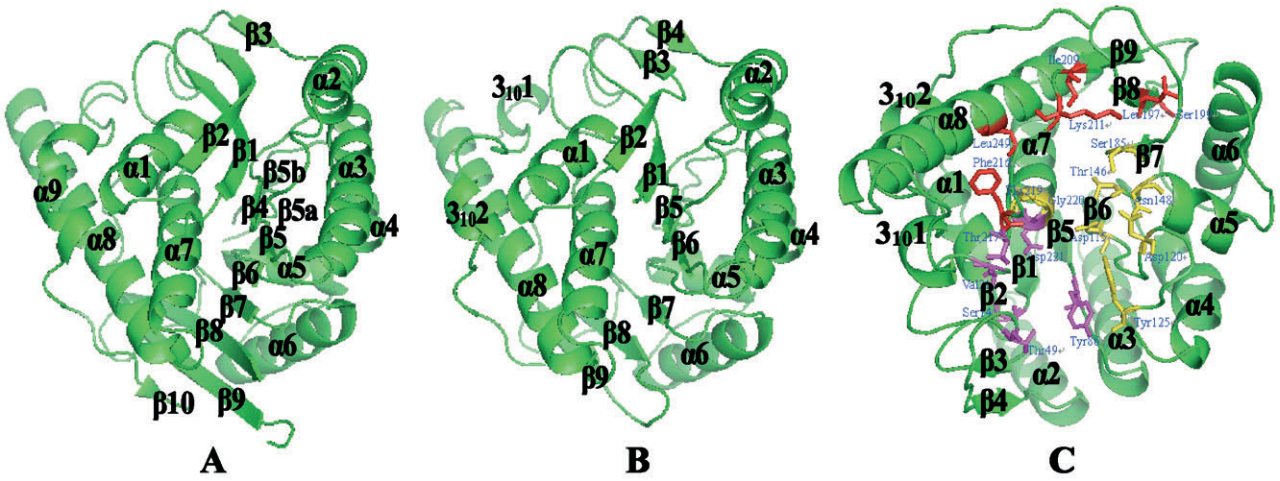

Fig. 13. A – Monomer structure of human PLK obtained from PDB database with the help of visual software Pymol. B – Monomer structure of *B. mori* PLK predicted by homology modelling. C – Monomer structure of *B. mori* PLK with active site. The ATP phosphate group-binding site, ATP adenine ring-binding site and PL-binding site are coloured yellow, red and purple, respectively.

active monomers (Kwok et al., 1987). As in mammals, the *B. mori* PLK also may be a dimer with two identical subunits under native conditions. The monomer molecular mass of *B. mori* PLK, however, is 33.1 KDa and smaller than the mammalian counterpart.

Previous structural analysis of sheep brain PLK complexes reveals that there is a key 12-residue loop (Gly-117 to Val-128) over the active site, which has an important role in the catalytic process. After ATP binding, the loop partially covers the ATP-binding site and prevents the unproductive hydrolysis of ATP; when substrates are absent, the loop exhibits a different conformation and occupies neither the ATP-binding site nor the PL-binding site (Li et al., 2002, 2004; Tang et al., 2005). The conformation of the corresponding segment in human PLK is not a loop, but a β-strand/loop/β-strand flap (Cao et al., 2006). A multiple sequence alignment of PLKs from different species (Fig. 12) indicates that the key peptides in *B. mori* consist of eight residues, similar to that in plants and *E. coli*. It is suggested that the length and conformation of the peptide might serve as an indicator of where it is along the evolutionary pathway of the PLK family from simple to complex.

The structure of the PLK active site is well studied in mammals (Li et al., 2002, 2004; Cao et al., 2006). Shared by human and sheep, the residues that interact with the phosphate groups of ATP are Ser^{187}, Thr^{148}, Asp^{113}, Asn^{150}, Asp^{118}, Gly^{234}, Tyr^{127} and Thr^{233}. The residue Tyr^{84} is on one side of the pyridine ring of PL and makes a π-interaction with the pyridine ring, whereas Val^{231} and Val^{19} are on the other side, interacting with PL by a hydrophobic effect. The N-1, O-3 and O-5 atoms of PL form hydrogen bonds and hydrophobic interact with the side chains of Ser^{12}, Thr^{47} and Asp^{235}, respectively. Residues Val^{41}, Phe^{43}, Val^{14}, Val^{56}, Trp^{52} and Val^{115} all contribute to forming a hydrophobic environment for the binding of PL to the active site; especially Tyr^{84}, Asp^{235} and Ser^{12}, share the function of determining substrate specificity. All of these important residues are found to be conserved in *B. mori* PLK, except Val^{231} and Trp^{52}. The residue Val is replaced by Thr in plants and *B.mori* PLK, whereas Trp is replaced by Ile in *B. mori* PLK.

Residues Ala^{201}, Met^{223} and Met^{263}, which interact with the adenine ring of ATP in sheep brain PLK through hydrophobic interactions, are substituted, respectively, in human PLK by more hydrophobic amino acids Val^{201}, Ile^{223} and Leu^{263} (Cao et al., 2006). In *B. mori* PLK, the residues are replaced by Gly, Ile and Leu, respectively. It is suggested that like human PLK, *B. mori* PLK has more affinity with ATP than sheep PLK. In addition, Asn^{121}, which has a positive charge over the ATP-binding site in sheep brain PLK, is replaced by negative charged residue Asp^{121}, and the residue Arg^{120} in the key peptide loop of sheep brain PLK is replaced by Trp^{120} in human PLK (Cao et al., 2006). Two amino acid residue positions are found to be absent from *B. mori* PLK. Moreover, residue Asn^{45} in human PLK is conserved among all species aligned in this research, but is substituted by Thr in *B. mori* PLK. A key residue His^{59} in *E. coli* PLK, interacts with the aldehyde group at C-4 of PL and may also determine if residues from the key peptide loop can fill the active site in the absence of the substrate (Safo et al., 2006). The residue His is substituted by Ala in *B. mori* PLK.

In *E. coli*, the metal ion Mg^{2+} and K^+ are required for enzyme activity (Li et al., 2002; Safo et al., 2006). In contrast, Zn^{2+} and K^+ have been proposed to be the metal ions needed for the activity of both human PL and sheep PL kinases (Li et al., 2002). However, a more recent study of the human enzyme showed that at non-physiological concentrations of the substrate and/or at pH 6, at which the previous assays were performed, Zn^{2+} does stimulate activity (McCormick et al., 1961; White & Dempsey, 1970), but under physiological conditions at pH 7.3, Mg^{2+} is the required divalent metal ion and Zn^{2+} inhibits the reaction (Di Salvo et al., 2004). At saturating PL and ATP concentrations, both Na^+ and K^+ activate human PLK, with Na^+ resulting in a six-fold increase in activity

TABLE 4. Genomic organization of *B. mori*, human, *A. thaliana*, malarial parasite and *E. coli* PLKs.

Species	Accession number	Chromosomal localization	Span (pb)	Exon (pb)	Exon (piece)	cDNA (pb)	Open reading frame (pb)	Amno acid
B. mori	DQ452397	8	7729	993	5	915	897	298
Human*	NM_003681.4	21	43000	7366	11	1210	939	312
*A. thaliana**	AF400125.1/AF404865	5	3428	–	13	930	930	309
Malaria parasite*	NP_7038201.1	6	1773	1494	3	1494	1494	497
*E. coli**	AP009048.1	–	852	852	–	852	852	283

* Data from NCBI database (http://www.ncbi.nlm.nih.gov/)

and K^+ only a 2.5-fold increase (Musayev et al., 2007). When the activity of the recombinant *B. mori* PLK using monovalent cations under saturating PL and ATP concentrations was measured it was found that K^+ is also an activator of the enzyme, whereas Na^+ did not activate PLK. The pH dependent study with Mg^{2+} and Zn^{2+} showed optimum enzyme activity at pH 6.0 and 5.5, respectively, with the Zn enzyme exhibiting more activity. At pH 7.3 with triethanolamine buffer, Zn^{2+} was still the most effective divalent cation for the catalysis of *B. mori* PLK. This data suggest that the optimal activity of *B. mori* PLK is recorded in acidic environments. Under physiological substrate concentrations, Mg^{2+} slightly stimulated the activity of *B. mori* PLK. It was not possible to detect inhibition by Zn^{2+} because the substrate concentrations were so low that the initial velocity could not be measured accurately. The mechanism of phosphorylation has been elucidated for sheep and *E. coli* enzymes, and follows a random sequential substrate addition (Li et al., 2002, 2004; Safo et al., 2004, 2006). Using PL as the variable substrate and ATP as the fixed substrate, a double reciprocal plot of initial velocity also suggests a sequential catalytic mechanism for the *B. mori* PLK.

Each human PLK monomer contains nine α-helices and 12 β-strands (Cao et al., 2006) (Fig. 13 A). Sheep brain PLK monomer contains 9 α-helices, 10 β-strands and 3 segments of 3_{10} helices (Li et al., 2002). The monomer of PLK from a prokaryote cell encoded by a *pdxK* gene consists of eight α-helices and nine ß-strands (Safo et al., 2006). It is hypothesized, based on homology modelling, that the *B. mori* PLK monomer contains eight α-helices (α1-8), nine β-strands (β1-9) and two segments of 3_{10} helices.

Table 4 summarizes the genomic organization of PLKs from *B. mori*, human, *A. thaliana*, malarial parasite and *E. coli*. The human *PLK* gene and that of *A. thaliana* contain more than ten exons, and that of *B. mori* and the malarial parasite five and three exons, respectively. The *B. mori PLK* gene has shorter introns than the human PLK gene. These differences may be related to the evolution of the PLK family and the complexity of the regulation of *PLK* gene expression.

In conclusion, the results of recombinant expression, purification and characterization of *B. mori* PLK are presented. This is the first report on the characterization of a PLK in insects. *B. mori* PLK contains signature-conserved amino acid sequence motifs of the PLK family. The catalytic properties and protein structure of *B. mori* PLK are similar to those of human PLK in terms of mass, but some distinguishing feature of the PLK was also observed in this study.

ACKNOWLEDGMENTS. This study was funded by the National Natural Science Foundation of China (No. 30870338).

REFERENCES

CAO P., GONG Y., TANG L., LEUNG Y.C. & JIANG T. 2006: Crystal structure of human pyridoxal kinase. *J. Struct. Biol.* **154**: 327–332.

DI SALVO M.L., HUNT S. & SCHIRCH V. 2004: Expression, purification and kinetic constants for human and Escherichia coli pyridoxal kinases. *Protein Expr. Purif.* **36**: 300–306.

GAO Z.G., LAU C.K., LO SC., CHOI S.Y., CHURCHICH J.E. & KWOK E. 1998: Porcine pyridoxal kinase cDNA cloning, expression and confirmation of its primary sequence. *Int. J. Biochem. Cell Biol*. **30**: 1379–1388.

HANNA M.C., TURNER A.J. & KIRKNESS E.E. 1997: Human pyridoxal kinase. cDNA cloning, expression, and modulation by ligands of the benzodiazepine receptor. *J. Biol. Chem.* **272**: 10756–10760.

HUANG L.Q., ZHANG J.Y., HAYAKAWA T.S. & TSUGE H.H. 1998: Vitaminic response of the silkworm, Bombyx mori fed the synthetic diet with different amounts of pyridoxine. *J. Seric. Sci. Jpn* **67**: 9–15.

HUANG S.H., SHI R.J., ZHANG J.Y. & HUANG L.Q. 2009: Cloning and characterization of a pyridoxine 5'-phosphate oxidase from silkworm, Bombyx mori. *Insect Mol. Biol.* **18**: 365–371.

KERRY J.A. & KWOK E. 1986: Purification and characterization of pyridoxal kinase from human erythrocytes. *Prep. Biochem.* **16**: 199–216.

KERRY J.A., ROHDE M. & KWOK E. 1986: Brain pyridoxal kinase. Purification and characterization. *Eur. J. Biochem*. **158**: 581–585.

KWOK F. & CHURCHICH J.E. 1979: Brain pyridoxal kinase. purification, substrate specificities, and sensitized photodestruction of an essential histidine. *J. Biol. Chem.* **254**: 6489–6495.

KWOK F., SCHOLZ G. & CHURCHICH J.E. 1987: Brain pyridoxal kinase dissociation of the dimeric structure and catalytic activity of the monomeric species. *Eur. J. Biochem.* **168**: 577–583.

LEE H.S., MOON B.J., CHOI S.Y. & KWON O.S. 2000: Human pyridoxal kinase: over expression and properties of the recombinant enzyme. *Mol. Cells* **10**: 452–459.

LI M.H., KWOK F., CHANG W.R., LAU C.K., ZHANG J.P., LO S.C.L., JIANG T. & LIANG D.C. 2002: Crystal structure of brain pyridoxal kinase, a novel member of the ribokinase superfamily. *J. Biol. Chem.* **277**: 46385–46390.

LI M.H., KWOK F., CHANG W.R., LAU C.K., LO S.C.L., ZHANG J.P., JIANG T. & LIANG D.C. 2004: Conformational changes in the reaction of pyridoxal kinase. *J. Biol. Chem.* **279**: 17459–17465.

LUM H.K., KWOK F. & LO S.C. 2002: Cloning and characterization of Arabidopsis thaliana pyridoxal kinase. *Planta* **215**: 870–879.

LUMENG L., LUI A. & LI T.K. 1980: Plasma content of b 6 vitamers and its relationship to hepatic vitamin b 6 metabolism. *J. Clin. Invest*. **66**: 688–695.

MARAS B., VALIANTE S., ORRU S., SIMMACO M., BARRA D. & CHURCHICH J.E. 1999: Structure of pyridoxal kinase from sheep brain and role of the tryptophanyl residues. *J. Protein Chem.* **18**: 259–268.

MCCORMICK D.B., GREGORY M.E. & SNELL E.E. 1961: Pyridoxal phosphokinases. 1. Assay, distribution, and properties. *J. Biol. Chem*. **236**: 2076–2084.

MERRILL A.H., HENDERSON J.M., WANG E., MCDONALD B.W. & MILLIKAN W.J. 1984: Metabolism of vitamin B_6 by human liver. *J. Nutr.* **114**: 1664–1674.

MUSAYEV F.N., DI SALVO M.L., KO T.P., GANDHI A.K., GOSWAMI Q. & SCHIRCH V. 2007: Crystal structure of human pyridoxal kinase: Structural basis of M^+ and M^{2+} activation. *Protein Sci.* **16**: 4542–4552.

SAFO M.K., MUSAYEV F.N., HUNT S., DI SALVO M.L., SCARSDALE N. & SCHIRCH V. 2004: Crystal structure of the pdxy protein from Escherichia coli. *J. Bacteriol.* **186**: 8074–8082.

SAFO M.K., MUSAYEV F.N., DI SALVO M.L., HUNT S., CLAUDE J.B. & SCHIRCH V. 2006: Crystal structure of pyridoxal kinase from the Escherichia coli pdxk gene: Implications for the classification of pyridoxal kinases. *J. Bacteriol.* **188**: 4542–4552.

SAKURAI T.H., OHKAW K. & MATSUDA M. 1993: Purification and properties of pyridoxal kinase from bovine brain. *Mol. Cell Biochem.* **119**: 203–207.

SCOTT T.C. & PHILLIPS M.A. 1997: Characterization of Trypanosome Brucei pyridoxal kinase: purification, gene isolation and expression in Escherichia coli. *Mol. Biochem. Parasitol.* **88**: 1–11.

SHI R.J., ZHANG J.Y., JIANG C.J. & HUANG L.Q. 2007: Bombyx mori pyridoxal kinase cDNA cloning and enzymatic characterization. *J. Genet. Genom.* **34**: 683–690.

TANG L., LI M.H., CAO P., WANG F., CHANG W.R., BACH S., REINHARDT J., FERANDIN Y., GALONS H., WAN Y., GRAY N., MEIJER L., JIANG T. & LIANG D.C. 2005: Crystal structure of pyridoxal kinase in complex with roscovitine and derivatives. *J. Biol. Chem.* **280**: 31220–31229.

WANG H., LIU D., LIU C. & ZHANG A. 2004: The pyridoxal kinase gene, TaPdxk from wheat complements vitamin B_6 synthesis-defective Escherichia coli. *J. Plant Physiol*. **161**: 1053–l060.

WHITE R.S. & DEMPSEY W.B. 1970: Purification and properties of vitamin B_6 kinase from Escherichia coli B. *Biochemistry* **9**: 4057–4064.

YANG Y., ZHAO G. & WINKLER M.E. 1996: Identification of the pdxK gene that encodes pyridoxine (vitamin B_6) kinase in Escherichia coli k-12. *FEMS Microbiol. Lett*. **141**: 89–95.

YANG Y., TSUI H.C., MAN T.K. & WINKLER M.E. 1998: Identification and function of the pdxY gene, which encodes a novel pyridoxal kinase involved in the salvage pathway of pyridoxal 5'phosphate biosynthesis in Escherichia coli k-12. *J. Bacteriol.* **180**: 1814–1821.

ZHANG J.Y. & HUANG L.Q. 2003: Distribution, movement and metabolism of vitamin B_6 compounds in the silkworm, Bombyx mori. *Acta Entomol. Sin.* **46**: 277–281 [in Chinese with English abstr.].

ZHANG Y., DOUGHERTY M., DOWNS D.M. & EALICK S.E. 2004: Crystal structure of an aminoimidazole riboside kinase from Salmonella enterica: implications for the evolution of the ribokinase superfamily. *Structure* **12**: 1809–1821.

Received February 10, 2010; revised and accepted July 7, 2010